university of groningen

University Medical Center Groningen

University of Groningen

SPECT and PET in Sympathetic Innervation

Noordzij, Walter

IMPORTANT NOTE: You are advised to consult the publisher's version (publisher's PDF) if you wish to cite from it. Please check the document version below.

Document Version
Publisher's PDF, also known as Version of record

Publication date:
2015

Link to publication in University of Groningen/UMCG research database

Citation for published version (APA):
Noordzij, W. (2015). *SPECT and PET in Sympathetic Innervation*. [S.n.].

Copyright
Other than for strictly personal use, it is not permitted to download or to forward/distribute the text or part of it without the consent of the author(s) and/or copyright holder(s), unless the work is under an open content license (like Creative Commons).

Take-down policy
If you believe that this document breaches copyright please contact us providing details, and we will remove access to the work immediately and investigate your claim.

Downloaded from the University of Groningen/UMCG research database (Pure): http://www.rug.nl/research/portal. For technical reasons the number of authors shown on this cover page is limited to 10 maximum.

Download date: 19-09-2021

CHAPTER 5

Sympathetic denervation in patients with ischemic cardiomyopathy and risk on ventricular tachy-arrhythmias. A pilot study.

Walter Noordzij[1], Arif Elvan[2], Fatma Demirel[2], Piet L. Jager[3], René A. Tio4, Riemer H.J.A. Slart[1]

[1] Department of Nuclear Medicine and Molecular Imaging, [4] Department of Cardiology, University of Groningen, University Medical Center Groningen, The Netherlands

[2] Department of Cardiology, [3] Department of Nuclear Medicine, Isala Hospital, Zwolle, The Netherlands

Submitted

ABSTRACT

Introduction: Patients with ischemic cardiomyopathy (ICM) are at risk for ventricular arrhythmias and are protected by an implantable cardioverter defibrillator (ICD). Visualization of cardiac sympathetic innervation may play an additional role to left ventricular ejection fraction (LVEF) in identifying those patients who will benefit from ICD therapy. The purpose of this study was to detect the role of sympathetic denervation in the genesis of ventricular arrhythmias in ICM patients.

Methods: 20 patients with ICM and LVEF < 30% were included in this pilot study. Included patients were equally stratified into two groups: no history of arrhythmias (group A) and recurrent arrhythmias (group B). All patients underwent cardiac sympathetic denervation (using carbon-11 labelled meta-hydroxy-ephedrine ([^{11}C]-mHED)), myocardial ischemia and viability detection. Patients were followed up to one year after the imaging studies.

Results: Mean age was 63 ± 7.5 years. Mean global retention of [^{11}C]-mHED was 0.055 ± 0,012 min^{-1}, and was not different between the two patient groups: 0.056 ± 0.011 min^{-1} vs 0.054 ± 0.013 min^{-1} for group A vs group B, respectively. During follow-up, seven patients developed ventricular arrhythmias, and four patients died. No difference in [^{11}C]-mHED retention was found between patients with and without ventricular arrhythmia during follow up. However, size of denervated area was larger in patients who died during follow up: 10 ± 1 segments vs 6 ± 2 segments, p = 0.002.

Conclusion: Cardiac sympathetic innervation is impaired in patients with ischemic cardiomyopathy. All-cause mortality occurred in those patients with large areas of [^{11}C]-mHED defect.

INTRODUCTION

Myocardial infarction results in nerve injury, followed by sympathetic nerve sprouting and regional heterogeneous myocardial hyperinnervation, stimulated by adjacent borderline ischemia (1,2). The coupling between augmented sympathetic nerve sprouting and electrically remodelled myocardium may result in ventricular tachycardia, ventricular fibrillation and sudden cardiac death (1,3,4). However, the exact role of sympathetic denervation and/or heterogeneous innervation in the genesis of these arrhythmias is yet not completely understood.

Patients with increased risk on ventricular arrhythmias, and severely reduced left ventricular ejection fraction (LVEF) of <35% will be protected by an implantable cardioverter defibrillator (ICD) (5). However, most of these patients will never develop fatal ventricular arrhythmias. A more accurate method to select patients for ICD indication is needed. Imaging of the sympathetic neurons involves radiolabelling of true adrenergic neurotransmitters or synthesis of radiolabelled catecholamine analogues (6). Carbon-11 labelled meta-hydroxyephedrine ([^{11}C]-mHED is the most frequently used positron emission tomography (PET) tracer for mapping of sympathetic neurons in patients with ischemic cardiomyopathy (7-10). Distribution of [^{11}C]-mHED throughout left ventricular myocardium in healthy normal individuals is regionally homogeneous with high uptake in all myocardial segments (7). It is an accurate non-invasive method to quantify the activity and distribution of sympathetic innervation.

The purpose of this study was to detect the role of sympathetic denervation in the genesis of ventricular arrhythmias after myocardial infarction in patients with ischemic left ventricular dysfunction and an increased risk of sudden cardiac death. First aim was to perform a preliminary study to evaluate [^{11}C]-mHED uptake and distribution in infarcted and non-infarcted regions of the left ventricle in patients with high and low risk on ventricular arrhythmias. Second aim was to evaluate whether uptake and distribution of [^{11}C]-mHED differs between patients with high and low risk on ventricular arrhythmias.

MATERIALS AND METHODS

Patients

This pilot project was a prospective, observational cohort study, in which 20 patients were included. All patients were eligible to receive, or had already received an ICD because of underlying ischemic cardiomyopathy. Patients were recruited in the Isala Hospital in Zwolle. Excluded were patients with disorders known to be associated with cardiac sympathetic dysfunction (such as hypertrophic cardiomyopathy, Brugada syndrome, arrhythmogenic right ventricular dysplasia and Parkinson disease), patients using tricyclic antidepressant agents, and patients with heart failure and New York Heart Association (NYHA) class III/IV. All patients gave written informed consent to participate in the study. The study was approved by the local medical ethics committee.

Included patients were stratified into two groups. The first group (group A, n=10 patients) involved patients with ischemic heart disease and left ventricular dysfunction (LVEF< 30%, based on radionuclide ventriculography) and no history of ventricular arrhythmias. The second group (group B, n=10 patients) involved patients with ischemic heart disease and reduced left ventricle function (LVEF<30%, based on radionuclide ventriculography) and a history of recurrent ICD shock therapy due to VT/VF.

In all patients, myocardial ischemia and viability detection was clinically assessed in the Isala Hospital in Zwolle, using gated technetium-99m ([^{99m}Tc]) labelled tetrofosmin myocardial perfusion single photon emission computed tomography (MPS) and fluorine-18 labelled fluorodeoxyglucose ([^{18}F]-FDG) PET, respectively. Patients were transferred to the University Medical Center Groningen (UMCG) for the [^{11}C]-mHED PET scan, combined with rest myocardial perfusion using nitrogen-13 labelled ammonia ([^{13}N]-NH_3). Diuretics, B-blockers and Ca-antagonists were withdrawn 24 hours before the [^{11}C]-mHED PET scan.

Data acquisition and image analysis Isala Hospital, Zwolle

Myocardial perfusion: all patients underwent rest MPS using a dose of [^{99m}Tc]-tetrofosmin (standard 740 MBq, 1,000 MBq in patients > 100kg). Images were acquires 45-60 minutes after tracer injection. Patients were scanned using a hybrid 64-slice SPECT/CT device (Ventri, GE Healthcare). Images were acquired using a low-energy, high resolution collimator, a 20% symmetrical window at 140 keV, a 64 x 64 matrix, and elliptical orbit with step-and-shoot acquisition at 6° intervals over a 180° arc with 30 steps. All patients were imaged in supine position with arms placed above the head. Acquisition time was 15 minutes. Rest MPS was followed by unenhanced low-dose CT scan during breath-hold with the following scanning parameters: 5.0-mm slice thickness using a reconstruction algorithm with a 512x512 matrix, and 800 ms rotation times at 120 kV and 20 mA. Emission images as well as attenuation map data were entered into a dedicated reconstruction algorithm to

provide 3-D volume data (available in a Xeleris workstation, GE Healthcare). These were reoriented in the standard way and displayed in the three traditional cardiac axes.

Experienced nuclear cardiac readers non-blindly interpreted the images, including MPS polar maps. Segments were scored using a 20-segment model for the left ventricle using the following five-point scoring system: 0 normal, 1 equivocal, 2 moderate reduction in radiotracer uptake, 3 severe reduction in radiotracer uptake, and 4 no detectable tracer uptake in a segment (11,12). Perfusion defect (with a score ≥ 2) on rest MPS, persisting despite applying CT-based attenuation correction together with abnormal wall motions in the corresponding segments, was considered infarcted myocardial tissue.

Viability: all patients underwent gated [^{18}F]-FDG (200 MBq) PET/CT (Discovery 16 slice, GE Healthcare). To stimulate [^{18}F]-FDG uptake, patients were given 75 g of glucose orally just before scanning or were given 500 mg of acipimox (Nedios, Byk Pharmaceuticals, Zwanenburg, The Netherlands) orally 90 min before scanning to lower circulating free fatty acids (13). To prevent side effects of acipimox (e.g. skin rash), 250 mg of aspirin was administered orally 5 min before acipimox. Dynamic acquisition followed after 200 MBq of [^{18}F]-FDG was injected intravenously. The total [^{18}F]-FDG PET acquisition time was 40 min, with the last 20 min acquired in gated mode with 16 frames per cardiac cycle. The length of each gate was based on the current R-R interval. The R-R interval was allowed to vary by 10 %. Data were corrected for attenuation using a low-dose CT scan and were reconstructed using filtered back projection (Hann filter, 0.5 pixels/cycle).

Viable myocardium was defined as the extent of mismatching area between myocardial infarction on MPS and tracer uptake on [^{18}F]-FDG PET. Non-viable myocardial tissue was defined a matching defect on both MPS and [^{18}F]-FDG PET.

PET data acquisition and image analysis UMCG, Groningen

All patients underwent dynamic [^{13}N]-NH_3 and [^{11}C]-mHED PET scans using a 1-day protocol. Scans were performed on ECAT EXACT HR+ PET camera system (Siemens Medical System, Knoxville, Tennessee, U.S.A.). Before dynamic scanning, a transmission scan for attenuation correction according to standard procedures was performed, using a rotating rod source filled with Ga^{68}/Ge^{68}, which is incorporated in the PET camera

Myocardial perfusion: to assess myocardial perfusion, following the transmission scan 400 MBq of [13N]-NH3 was administered. Dynamic data of [13N]-NH3 were acquired over 15 minutes, followed by gated mode acquisition. This allowed quantification of perfusion at rest. The [^{13}N]-NH_3 emission data were corrected for attenuation and after reorientation, short-axis images of [^{13}N]-NH_3 were obtained with a plane thickness of about 7 mm at an in-plane resolution of approximately 7 mm. A fully automatic non-operator dependent program (MATLAB)

which incorporates spill-over correction was used to quantify the mean blood flow (MBF) of the segments of the left ventricle (mL/min/100g).

Sympathetic innervation: after injection of approximately 350 MBq (range 200-400 MBq) of [^{11}C]-mHED, dynamic imaging was performed for 60 minutes and heart rate and blood pressure were monitored continuously. The [^{11}C]-mHED emission data were corrected for attenuation and residual activity of the earlier [13N]-NH3 scan. For quantification, a retention index was calculated by dividing the mean myocardial radioactivity concentration in the last 20 minutes of the PET scan by the integral of the time-activity curve in arterial blood (derived from a region of interest in the right ventricular chamber). Images were reoriented to the long and short axes of the left ventricle using a special workstation. Gating files were processed in QGS software.

Data was collected and analysed at the nuclear medicine department of the UMCG. At a three month interval following ICD implantation, the device was interrogated to assess number of episodes of ventricular arrhythmias. The sympathetic uptake and distribution between both patient groups were compared. Infarcted myocardium was quantified from a mismatch analysis between [^{13}N]-NH_3 and [^{18}F]-FDG. Mean [^{11}C]-mHED retention (min^{-1}) was determined for those areas with both normal perfusion (>80% of the maximum myocardial blood flow) and innervation (>75% of the segment with maximum [^{11}C]-mHED retention), areas with a mismatch pattern: normal perfusion and decreased cardiac sympathetic innervation (<75% of the segment with maximum [^{11}C]-mHED retention), and both abnormal perfusion (<80% of the maximum myocardial blood flow) and innervation. The follow up of the patients after the PET scan was one year.

Statistical analysis

Baseline descriptive statistics are presented as mean ± standard deviation or median (range) for continuous variables and numbers with percentages for categorical variables as required. We evaluated differences between the two study groups using the χ^2 test and Fisher's exact test for categorical data and the Student's *t*-test and Mann–Whitney *U* test for continuous data, according to whether data were normally distributed. In all analyses, $P < 0.05$ was considered statistically significant. Statistical analysis was performed using the SPSS package version 22 (IBM Corp., Armonk, NY, USA).

RESULTS

Patient characteristics

The baseline characteristics of the patients are summarized in Table 1. Nearly all patients were male; only one female patient was included. The mean age was 63 ± 7.5 years. There was no significant difference in age between patients with low versus high risk of arrhythmia: 61 ± 5.9 vs 66 ± 8.3 years, respectively. All patients had a history of acute myocardial infarction. The inferior LV wall was mostly frequently: in 11 of the 20 patients. Both groups had an equal number of patients who previously underwent percutaneous coronary intervention (PCI) or coronary artery bypass grafting (CABG). Traditional risk factors for coronary artery disease were present in a minority of the patients, and were equally distributed over both patient groups. The majority of the patients used beta blockers, oral anticoagulants, angiotensin converting enzyme inhibitors (ACE-i), diuretics and cholesterol lowering agents (statins).

Viability detection

The results of myocardial perfusion SPECT are summarized in Table 2. All patients had signs of infarcted myocardium on myocardial perfusion SPECT. LVEF in all patients was severely reduced. The high risk group showed lower LVEF than the low risk patients (25 ± 5.9 % vs 35 ± 7.4 %, $p = 0.016$). End diastolic and end systolic volumes were significantly higher in high risk group, compared to the low risk group. All patients showed a defect on cardiac [^{18}F]-FDG imaging, at the area of the perfusion defect on perfusion SPECT. However, in three patients the defect in [^{18}F]-FDG uptake was less pronounced than the perfusion defect, indicating some viability of the affected myocardial wall segments.

Cardiac sympathetic innervation

Table 3 shows the results of the [^{11}C]-mHED scans. Mean global retention of [^{11}C]-mHED was 0.055 ± 0.012 min^{-1}, and was not different between the two patient groups: 0.056 ± 0.011 min^{-1} vs 0.054 ± 0.013 min^{-1} for low vs high risk patients, respectively. Mean [^{11}C]-mHED retention values were statistically different between normal perfusion-innervation, perfusion-innervation mismatch, and both abnormal perfusion and innervation patterns: 0.069 ± 0.016 min^{-1}, 0.048 ± 0.012 min^{-1} ($p <$ 0.001) and 0.037 ± 0.011 min^{-1} ($p < 0.001$), respectively (Figure 1). Mean [^{11}C]-mHED retention in mismatch areas was significantly lower in patients with high risk of arrhythmia compared to those with low risk: 0.044 ± 0.0086 min^{-1} vs 0.052 ± 0.015 min^{-1}, $p = 0.025$.

Table 1
Patient characteristics

	Frequency (*n*) or mean ± SD			
	All patients	**Low risk patients**	**High risk patients**	***p*-value**
Age (years)	63 ± 7.5	61 ± 5.9	66 ± 8.3	ns
Male (n)	19	9	10	ns
Medical history (*n*)				
Diabetes	2	1	1	ns
Hypertension	9	5	4	ns
Smoking	10	6	4	ns
Hypercholesterolemia	10	4	6	ns
Family history of CAD	6	4	2	ns
Previous PCI	12	6	6	ns
Previous CABG	14	7	7	ns
Previous VT or VF	6	3	3	ns
Medication at baseline (*n*)				
Oral anticoagulant	14	6	8	ns
Beta blocker	19	10	9	ns
Calcium antagonist	4	2	2	ns
ACE-i	15	6	9	ns
Diuretics	11	3	8	0,025
Statin	16	8	8	ns

PCI percutaneous coronary intervention, CAD coronary artery disease, CABG coronary artery bypass grafting, VT ventricular tachycardia, VF ventricular fibrillation, OAC oral anticoagulant, ACE-i angiotensin converting enzyme inhibitor.

Table 2
Myocardial perfusion SPECT results

	Frequency (*n*) or mean ± SD			
	All patients	**Low risk patients**	**High risk patients**	***p*-value**
EDV (mL)	210 ± 68.8	163 ± 30.8	267 ± 58.3	0.012
ESV (mL)	148 ± 65.5	103 ± 28.4	203 ± 54.7	0.011
LVEF (%)	31 ± 8.3	35 ± 7.4	25 ± 5.9	0.016

EDV end-diastolic volume, ESV end-systolic volume, LVEF left ventricular ejection fraction.

Table 3
[^{11}C]-mHED results

	Frequency (*n*) or mean ± SD			
	All patients	**Low risk patients**	**High risk patients**	***p*-value**
Mean ^{11}C-mHED retention (min^{-1})	0.055 ± 0.012	0.056 ± 0.011	0.054 ± 0.013	ns
Mismatch segments (*n*)	2.8 ± 1.7	2.6 ± 2.0	3.0 ± 1.3	ns
Abnormal segments (*n*)	5.2 ± 2.1	4.6 ± 2.5	5.7 ± 1.6	ns
Reversed mismatch segments (*n*)	3.2 ± 1.9	2.9 ± 1.5	3.4 ± 2.4	ns
Normal segments (*n*)	5.9 ± 2.0	6.9 ± 1.5	4.9 ± 2.0	0.02

Mismatch = segments with normal perfusion (>80% of maximum), and low mHED retention (<75% of maximum ^{11}C-mHED retention); abnormal = low perfusion and low mHED retention; reversed mismatch = low perfusion and normal mHED retention; normal = normal perfusion and normal mHED retention.

Figure 1
Mean [^{11}C]-mHED retention in the different perfusion-innervation patterns

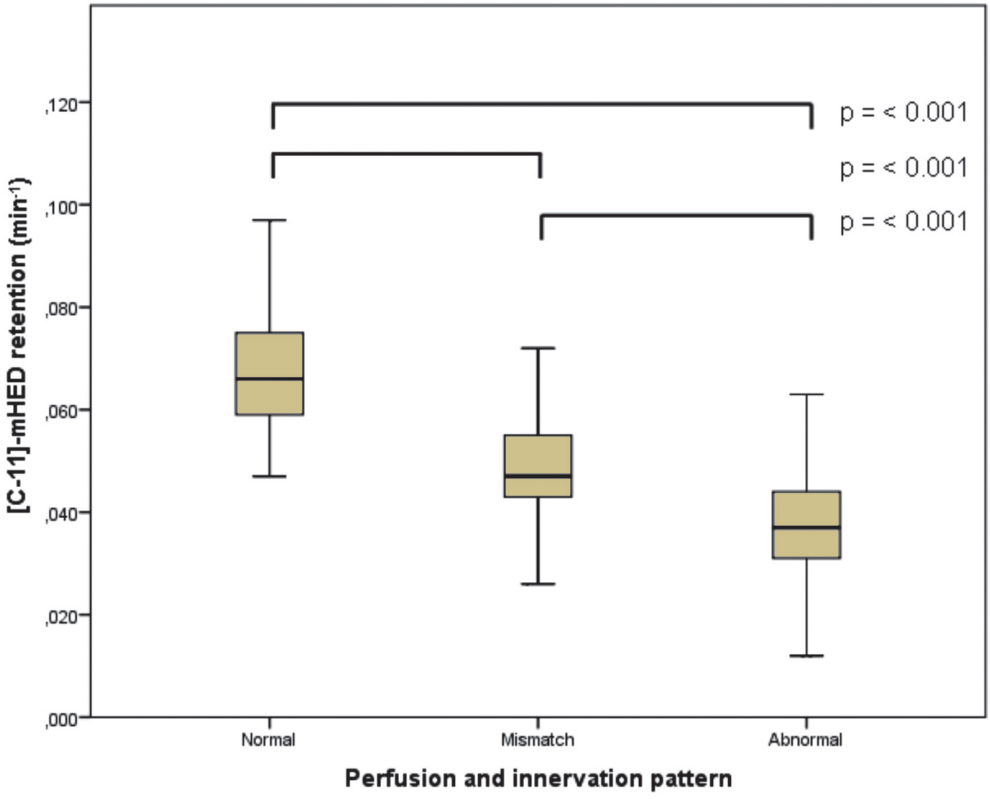

There was no difference in the number of segments with mismatch patterns between patient groups. Neither could we find a difference in the number of segments with both abnormal blood flow and [^{11}C]-mHED retention, and segments with a reversed mismatch pattern. However, the number of segments with both normal blood flow and [^{11}C]-mHED retention was lower in the high risk group compared to the low risk group (4.9 ± 2.0 segments vs 6.9 ± 1.5 segments, p = 0.02).

When comparing the [^{11}C]-mHED data with the [^{18}F]-FDG results, all patients showed a matching pattern of low [^{11}C]-mHED retention at the sites of low [^{18}F]-FDG uptake (Figure 2). However, at the borders of the infarcted area, five patients had segments with normal [^{18}F]-FDG uptake and low [^{11}C]-mHED retention (viability-innervation mismatch pattern), and five other patients showed a reversed viability-innervation mismatch pattern (normal [^{11}C]-mHED retention and low [^{18}F]-FDG uptake). There was no correlation between the presence of either [^{11}C]-mHED - [^{18}F]-FDG mismatch or reversed mismatch on one hand, and the risk of arrhythmia on the other.

Figure 2

Bulls-eye plots of myocardial perfusion, denervation and viability imaging. (**A**) rest myocardial perfusion using [^{13}N]-NH_3 PET with a perfusion defect in the inferoseptal segments, (**B**) [^{11}C]-mHED showing a matched innervation defect in the inferoseptal segments, (**C**) [^{18}F]-FDG PET showing no viability of the inferoseptal segments

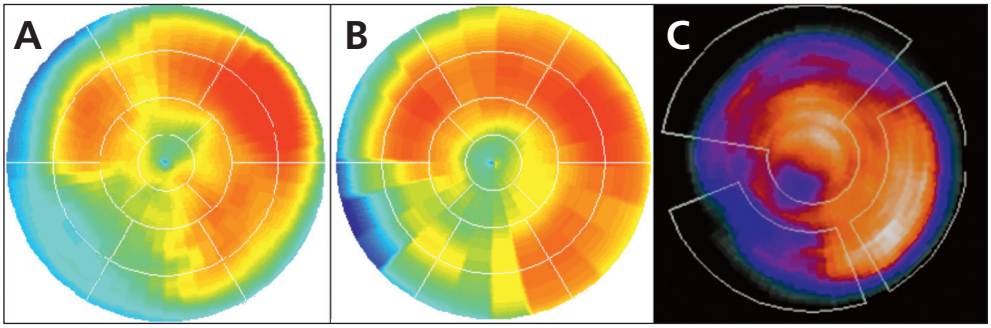

Follow up

During follow up, ventricular arrhythmia occurred in seven patients, more often in the high risk group than the low risk group: six patients vs one patient (p = 0.019, Table 4). Antitachycardia pacing occurred in four patients who developed VT and VF. All of these patients showed multiple episodes of VT or VF. Two of these four patients also received an appropriate shock. Two patients received an appropriate shock without preceding antitachycardia pacing. Eventually four patients died during follow up. Mean overall time to follow up was 74 ± 29 months, and was not different between low and high risk patients.

There was no difference in [^{11}C]-mHED retention between patients with and without ventricular arrhythmia during follow up. There was also no difference in the presence of either [^{11}C]-mHED - [^{18}F]-FDG mismatch or reversed mismatch between the patients developing arrhythmia and those without arrhythmia during follow up. However, the size of denervated area on [^{11}C]-mHED was larger in patients who died during follow up: 10 ± 1 segments vs 6 ± 2 segments (p = 0.002).

DISCUSSION

Our results suggest that the extent of denervated myocardium on [^{11}C]-mHED PET in patients with ischemic cardiomyopathy are associated with a higher frequency of all-cause mortality. We did not find a relationship between a history of VT or VF after myocardial infarction and the presence or size of denervated myocardium. Neither a relationship between the presence of myocardial denervation and the occurrence of ventricular arrhythmia was found during follow up. However, the stratification of patients between low and risk of developing ventricular arrhythmia seems to be a good predictor for the actual occurrence of VT of VF during follow up.

A previous PET study described significant lower [^{11}C]-mHED uptake in perfusion-innervation matched defects and perfusion-innervation mismatch (normal flow and decreased innervation), compared to matched normal perfusion-innervation areas in patients with an acute myocardial infarction (8). Although all patients underwent revascularization, there was no sign of reinnervation in any of these patients after 8 months of follow up, a finding also observed in a later study (14). It suggests persisting neuronal damage of (peri-) infarcted myocardial tissue, which can be confirmed by our results.

In a later study, patients with coronary artery disease, but without a history of myocardial infarction, underwent both [^{11}C]-mHED and [^{13}N]-NH_3 PET scans (15). Cardiac sympathetic denervation was found in a majority of the areas with normal resting myocardial blood flow. Coronary artery disease (CAD) - defined as ≥90% stenosis of native vessel / post CABG, ischemia, or post PCI - was present more often in those areas with low than in areas with normal [^{11}C]-mHED uptake. This finding suggested higher susceptibility of sympathetic nerves to ischemia compared to cardiomyocytes. However, also the opposite seems to be true according to a group of 27 CAD patients, in which cardiac sympathetic innervation was preserved in areas with reduced myocardial blood flow (16).

In the most recent study using [^{11}C]-mHED in ischemic cardiomyopathy, patients also underwent [^{13}N]-NH_3 and [^{18}F]-FDG PET scans (10). All 204 included patients were eligible for an ICD, based on a history of myocardial infarction and LVEF ≤ 35%. Patients were followed every three months, with a median follow up of more than four years (range 2.5 - 7.2 years). Primary endpoint was sudden cardiac arrest (SCA), defined as arrhythmic death or ICD discharge for VF or VT > 240 beats / minute. Multivariate analysis showed that time to SCA was dependant on the size of denervated myocardium, LV end-diastolic volume, serum creatinine level and the absence of ACE-i. In concordance to our study, neither the volume of hibernating myocardium nor the volume of infarcted tissue was associated with mortality, suggesting that these parameters are not useful in the prediction of developing SCA.

The results of the present study should be interpreted with caution. This pilot study included a small sample size of patients over a prolonged period of time. Although patients with ischemic cardiomyopathy have a higher risk of SCA, the frequency of arrhythmic death or ICD discharge because of VF or VT > 240/min in these twenty patients was relatively low.

The use of ACE-i is known to provide a cardioprotective effect for developing SCA, by means of reducing sympathetic hyperactivity (10). In this pilot study, the majority of patients used ACE-i (75%). During follow up, there was no difference in the frequency of ventricular arrhythmia in patients with or without angiotensin blockade.

Up to present, the choice for ICD implantation in patients with ischemic cardiomyopathy is based on LVEF < 35% (17). However, LVEF alone does not seem to be a good prognostic factor for successful ICD therapy (18). Cardiac sympathetic innervation imaging appears to be of prognostic value for survival, independently of LVEF and NYHA class (18, 19). Therefore, future studies should focus on the additional value of cardiac sympathetic innervation imaging in the clinical decision making for appropriate ICD therapy.

CONCLUSION

Cardiac sympathetic innervation is impaired in patients with ischemic cardiomyopathy. All-cause mortality occurred in those patients with large areas of [^{11}C]-mHED retention defect. According to this pilot study, the volume of infarcted tissue was not associated with mortality, suggesting that this parameter is not useful in the prediction of developing SCA.

ACKNOWLEDGEMENTS

We would like to thank Didy Markies-Bremer, research nurse from Diagram BV, for her contribution in patient recruitment.

REFERENCES

1 Chen PS, Chen LS, Cao JM, Sharifi B, Karagueuzian HS, Fishbein MC. Sympathetic nerve sprouting, electrical remodeling and the mechanisms of sudden cardiac death. Cardiovasc Res. 2001;50:409-416

2 Zipes DP. Influence of myocardial ischemia and infarction on autonomic innervation of the heart. Circulation. 1990; 82:1095-1105

3 Cao JM, Chen LS, KenKnight BH, Ohara T, Lee MH, Tsai J, Lai WW, Karagueuzian HS, Wolf PL, Fishbein MC, Chen PS. Nerve sprouting and sudden cardiac death. Circ Res. 2000;86:816-821

4 Du XJ, Cox HS, Dart AM, Esler MD. Sympathetic activation triggers ventricular arrhythmias in rat heart with chronic infarction and failure. Cardiovasc Res. 1999;43:919-929

5 Moss AJ, Zareba W, Hall WJ, Klein H, Wilber DJ, Cannom DS, Daubert JP, Higgins SL, Brown MW, Andrews ML; Multicenter Automatic Defibrillator Implantation Trial II Investigators. Prophylactic implantation of a defibrillator in patients with myocardial infarction and reduced ejection fraction. N Engl J Med 2002;346:877–883

6 Bengel FM, Schwaiger M. Assessment of cardiac sympathetic neuronal function using PET imaging. J Nucl Cardiol. 2004;11: 603-616

7 Rosenspire KC, Haka MS, Van Dort ME, Jewett DM, Gildersleeve DL, Schwaiger M, Wieland DM. Synthesis and preliminary evaluation of carbon-11-meta-hydroxyephedrine: a false transmitter agent for heart neuronal imaging. J Nucl Med. 1990;31:1328-1334

8 Allman KC, Wieland DM, Muzik O, Degrado TR, Wolfe ER Jr, Schwaiger M. Carbon-11 hydroxyephedrine with positron emission tomography for serial assessment of cardiac adrenergic neuronal function after acute myocardial infarction in humans. J Am Coll Cardiol. 1993;22:368-375

9 Fallen EL, Coates G, Nahmias C, Chirakal R, Beanlands R, Wahl L, Woodcock G, Thomson M, Kamath M. Recovery rates of regional sympathetic reinnervation and myocardial blood flow after acute myocardial infarction. Am Heart J. 1999;137:863-869

10 Fallavollita JA, Heavey BM, Luisi AJ Jr, Michalek SM, Baldwa S, Mashtare TL Jr, Hutson AD, Dekemp RA, Haka MS, Sajjad M, Cimato TR, Curtis AB, Cain ME, Canty JM Jr. Regional myocardial sympathetic denervation predicts the risk of sudden cardiac arrest in ischemic cardiomyopathy. J Am Coll Cardiol. 2014;63:141-149

11 Berman DS, Kiat H, van Train K, Garcia E, Friedman J, Maddahi J. Technetium 99m sestamibi in the assessment of chronic coronary artery disease. Semin Nucl Med. 1991;21:190–212

12 Berman DS, Kiat H, Friedman JD, Wang FP, van Train K, Matzer L, et al. Separate acquisition rest thallium-201/stress technetium-99m sestamibi dual isotope myocardial perfusion single-photon emission computed tomography: a clinical validation study. J Am Coll Cardiol. 1993;22:1455–1464

13 Knuuti MJ, Yki-Järvinen H, Voipio-Pulkki LM, Mäki M, Ruotsalainen U, Härkönen R, et al. Enhancement of myocardial [fluorine-18]fluorodeoxyglucose uptake by a nicotinic acid derivative. J Nucl Med 1994;35:989–998

14 Fricke E, Eckert S, Dongas A, Fricke H, Preuss R, Lindner O, Horstkotte D, Burchert W. Myocardial sympathetic innervation in patients with symptomatic coronary artery disease: follow-up after 1 year with neurostimulation. J Nucl Med. 2008;49:1458-1464

15 Bulow HP, Stahl F, Lauer B, Nekolla SG, Schuler G, Schwaiger M, Bengel FM. Alterations of myocardial presynaptic sympathetic innervation in patients with multi-vessel coronary artery disease but without history of myocardial infarction. Nucl Med Commun. 2003;24:233-239

16 Fricke E, Fricke H, Eckert S, Zijlstra S, Weise R, Lindner O, Horstkotte D, Burchert W. Myocardial sympathetic innervation in patients with chronic coronary artery disease: is reduction in coronary flow reserve correlated with sympathetic denervation? Eur J Nucl Med Mol Imaging. 2007;34:206-211

17 McMurray JJ, Adamopoulos S, Anker SD, Auricchio A, Böhm M, Dickstein K, Falk V, Filippatos G, Fonseca C, Gomez-Sanchez MA, Jaarsma T, Køber L, Lip GY, Maggioni AP, Parkhomenko A, Pieske BM, Popescu BA, Rønnevik PK, Rutten FH, Schwitter J, Seferovic P, Stepinska J, Trindade PT, Voors AA, Zannad F, Zeiher A; ESC Committee for Practice Guidelines. ESC Guidelines for the diagnosis and treatment of acute and chronic heart failure 2012: The Task Force for the Diagnosis and Treatment of Acute and Chronic Heart Failure 2012 of the European Society of Cardiology. Developed in collaboration with the Heart Failure Association (HFA) of the ESC. Eur Heart J. 2012;33:1787-1847

18 Nakata T, Nakajima K, Yamashina S, Yamada T, Momose M, Kasama S, Matsui T, Matsuo S, Travin MI, Jacobson AF. A pooled analysis of multicenter cohort studies of (123)I-mIBG imaging of sympathetic innervation for assessment of long-term prognosis in heart failure. JACC Cardiovasc Imaging. 2013;6:772-784

19 Shah AM, Bourgoun M, Narula J, Jacobson AF, Solomon SD. Influence of ejection fraction on the prognostic value of sympathetic innervation imaging with iodine-123 MIBG in heart failure. JACC Cardiovasc Imaging. 2012;5:1139-1146